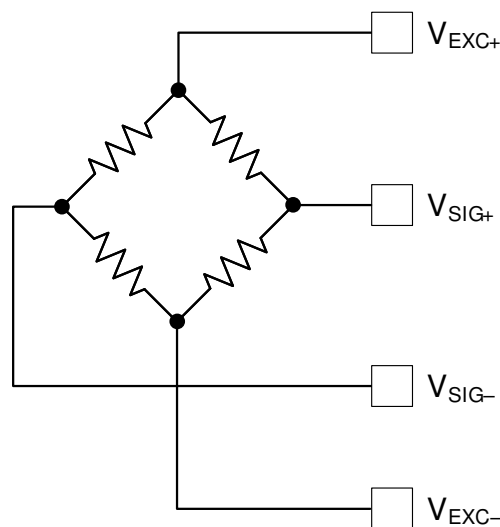


# Reduce Bridge Measurement Offset and Drift Using the AC Excitation Mode in the ADS1235 and ADS1261



## Introduction

Many industrial end-equipment employ resistive bridges to sense changes in physical variables such as strain, force, pressure, temperature, or flow rates. A common industrial application for resistive bridges is precision [weigh scales](#). In this application, weight is translated into a voltage using a resistive bridge embedded in a load cell similar to [Figure 1](#).



**Figure 1. Resistive Bridge in a Load Cell**

The 4-wire load cell shown in [Figure 1](#) requires an excitation voltage,  $V_{EXC\pm}$ , and outputs a differential signal voltage,  $V_{SIG\pm}$ , proportional to the applied weight. Typically,  $V_{SIG\pm}$  (max) is on the order of tens of millivolts, requiring a low-noise, [precision delta-sigma ADC](#) with an integrated gain stage to provide repeatable measurements for such low-level signals.

ADC accuracy parameters such as offset error, offset drift, gain error and gain drift are important to ensure the weigh scale output correlates to the correct weight. To meet the demanding performance needs of precision bridge measurements, Texas Instruments offers the [ADS1235](#), a 24-bit, 7.2-kSPS, 6-channel delta-sigma ADC, as well as the [ADS1261](#), a 24-bit, 40-kSPS, 10-channel, delta-sigma ADC. Both of these ADCs incorporate several features necessary for precision bridge measurements, including:

1. **Integrated PGA** – the ADS1261 provides all binary gains from 1 to 128 while the ADS1235 offers gain values of 1, 64, and 128, enabling input-referred noise as low as 6 nV<sub>RMS</sub>
2. **Differential voltage reference inputs** – enables ratiometric measurements that provide the lowest-noise signal acquisition
3. **AC excitation control signals** – use with external switches to swap bridge excitation polarity to reduce offset and offset drift

This document focuses on AC excitation to demonstrate why it is important and how it works using the ADS1235 and ADS1261. The subsequent sections only reference the ADS1235 because the same principles and operation generally apply to the ADS1261. However, should any relevant differences exist between these ADCs, they are noted.

## What is AC Excitation?

While some ADCs, including the ADS1235, integrate chopping techniques to reduce *device* offset, these methods only reduce those errors that occur after the chopping circuitry. Therefore, any offset prior to the input of the device can still degrade measurement accuracy.

AC excitation, or bridge chopping, helps solve this design challenge by reducing *system-level* offset errors from a bridge measurement. Reducing the system offset also reduces system offset drift, an error term that is not easily removed by calibration.

The AC excitation method described in this document uses external switches to alternate the bridge excitation polarity, and should not be confused with excitation using a true AC signal. Instead, the system averages one forward-polarity and one reverse-polarity measurement to yield a single conversion result that is virtually offset-free.

## Typical AC Excitation Circuit Using the ADS1235

Figure 2 depicts a simplified connection diagram for a typical 4-wire AC excitation circuit using the ADS1235.

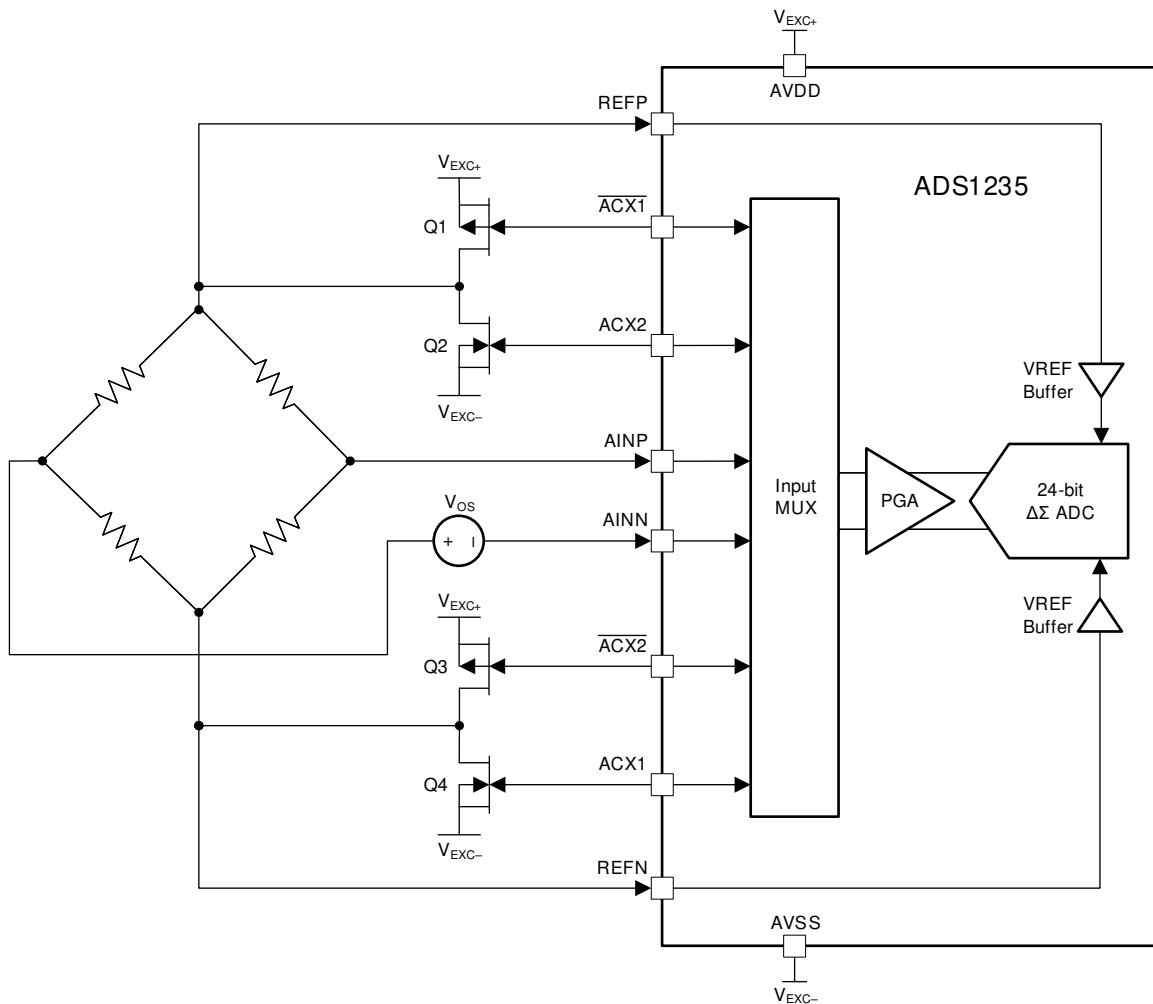


**Figure 2. Four-Wire AC Excitation Circuit Using ADS1235**

Figure 2 employs two P-channel MOSFETs and two N-channel MOSFETs to forward and reverse bias the bridge. These MOSFETs are controlled by specific ADC pins:  $\overline{ACX1}$ ,  $\overline{ACX2}$ , ACX1, and ACX2. The timing and logic levels of each signal must be tightly controlled to switch the MOSFETs effectively. Figure 3 shows the timing diagram for the ADS1235 ACX pins.

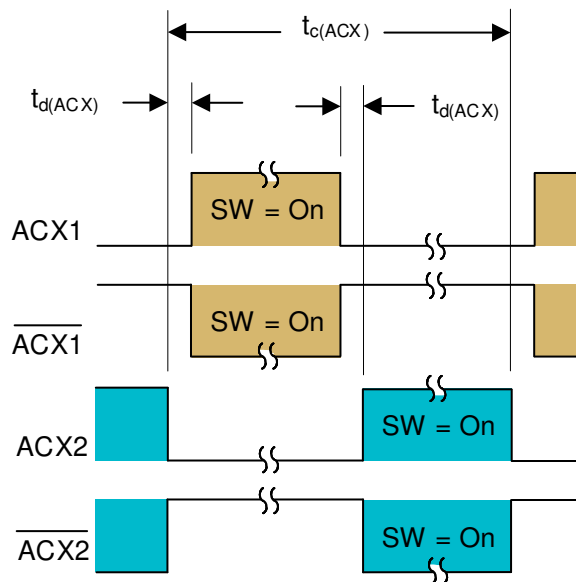


Figure 3. ADS1235 AC Excitation Signal Timing Diagram

The orange highlights in Figure 3 denote when the MOSFETs (Q1 and Q4) are enabled during the forward-polarity phase, while the blue highlights indicate when the MOSFETs (Q2 and Q3) conduct during the reverse-polarity phase. Importantly, the delay,  $t_{d(ACX)}$ , between the ON-time for each switch avoids any MOSFET shoot-through current that results if both a P-channel and N-channel device are on simultaneously.

The logic levels on the ADS1235 ACX pins are referenced to the ADC analog supply (AVDD), not the digital supply (DVDD) as some might expect, due to the following system factors:

- Resistive bridge measurements typically operate with  $V_{EXC} = 5\text{ V}$  to maximize dynamic range
- AVDD on the ADS1235 is restricted to 5 V
- $V_{EXC}$  is commonly shared with AVDD and AVSS (see Figure 2) as long as doing so does not violate the ADC operating conditions

As a result of these three factors, the ACX pins must use 5-V logic levels to sufficiently control the MOSFETs in the system shown in Figure 2, which is why these pins are referenced to AVDD.

#### How does AC excitation improve system accuracy?

AC excitation averages two consecutive measurements,  $V_{PHASE1}$  and  $V_{PHASE2}$ , to remove offset error. Equation 1 calculates the combined conversion result.

$$V_{CONV\_RESULT} = (V_{PHASE1} - V_{PHASE2}) / 2 \quad (1)$$

Figure 4 shows the connection diagrams and the excitation voltage path for both the Phase 1 (Figure 4A) and Phase 2 (Figure 4B) measurements.

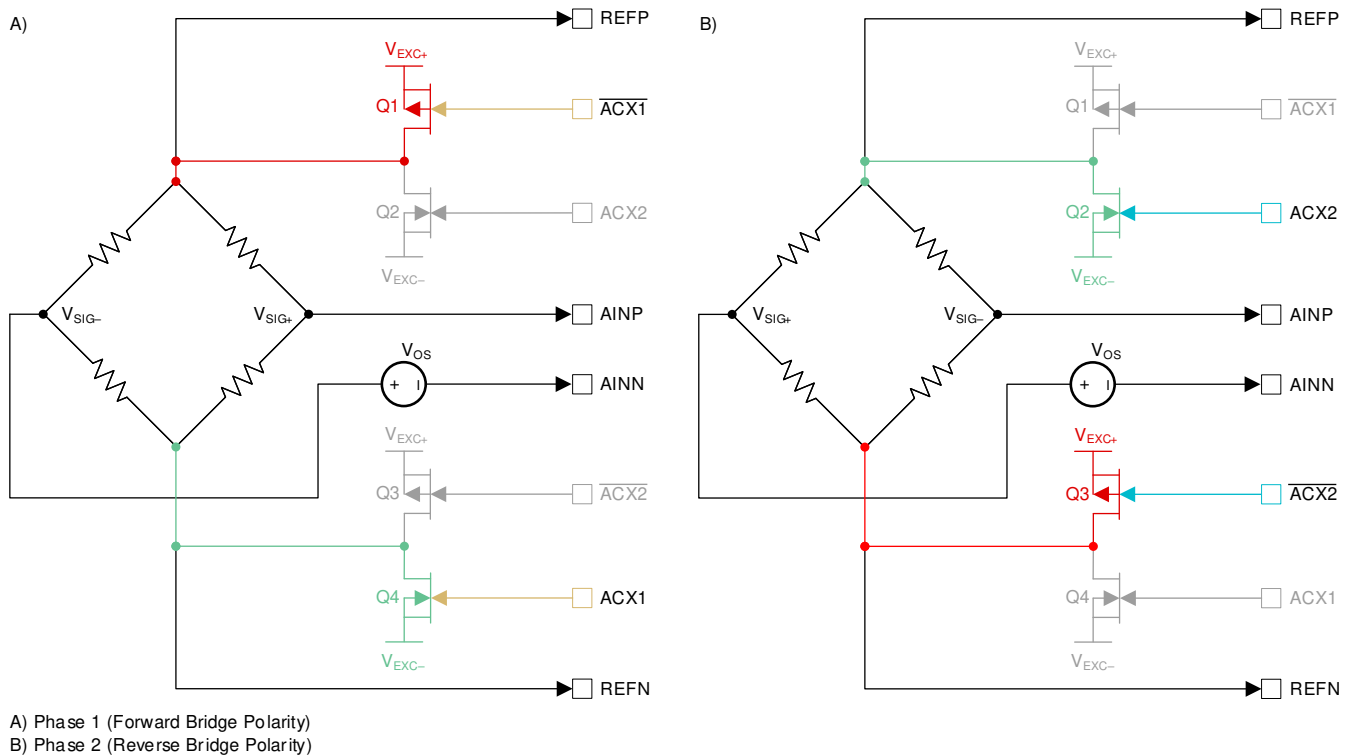


**Figure 4. AC Excitation Connection Diagrams: Phase 1 (Left) and Phase 2 (Right)**

In Phase 1 of the AC excitation mode of the ADS1261 (see Figure 4A), the ACX1 and  $\overline{\text{ACX1}}$  outputs are enabled such that  $V_{\text{EXC}+}$  connects to the top of the bridge and  $V_{\text{EXC}-}$  connects to the bottom of the bridge. As highlighted in orange in the timing diagram in Figure 3,  $\overline{\text{ACX1}}$  is at logic low (0 V) and ACX1 is at logic high (5 V) during the forward-polarity phase. With  $\overline{\text{ACX1}}$  at 0 V, the gate-source voltage,  $V_{\text{GS}}$ , is  $< 0$  V, which turns Q1 on. Similarly, ACX1 at 5 V sets  $V_{\text{GS}} > 0$  for Q4, which turns Q4 on as well. The opposite is true for Q2 and Q3 such that both of these devices do not conduct.

Equation 2 shows  $V_{\text{PHASE1}}$  in terms of  $V_{\text{SIG}\pm}$  as well as the offset term,  $V_{\text{OS}}$ , which represents all offsets in the measurement system.

$$V_{\text{PHASE1}} = V_{\text{SIG}+} - (V_{\text{SIG}-} + V_{\text{OS}}) \quad (2)$$

In Phase 2, the ACX outputs switch such that only the MOSFETs connected to ACX2 and  $\overline{\text{ACX2}}$  conduct. This configuration routes  $V_{\text{EXC}+}$  to the bottom of the bridge and  $V_{\text{EXC}-}$  to the top, reversing the polarity of the signal seen at the inputs of the ADC (AINN and AINP). Figure 4B shows this reverse-polarity configuration.

As highlighted in blue in the timing diagram in Figure 3,  $\overline{\text{ACX2}}$  is at logic low (0 V) and ACX2 is at logic high (5 V) during the reverse-polarity phase. With  $\overline{\text{ACX2}}$  at 0 V,  $V_{\text{GS}}$  is  $< 0$  V, which turns Q2 on. Similarly, ACX2 at 5 V sets  $V_{\text{GS}} > 0$  for Q3, which turns Q3 on as well. The opposite is true for Q1 and Q4 such that both of these devices do not conduct.

In the reverse-polarity configuration shown in Figure 4B,  $V_{\text{PHASE2}}$  is represented by Equation 3. Note that while the measurement polarity is reversed, the bridge offset polarity is the same.

$$V_{\text{PHASE2}} = V_{\text{SIG}-} - (V_{\text{SIG}+} + V_{\text{OS}}) \quad (3)$$

Replacing  $V_{PHASE1}$  and  $V_{PHASE2}$  from Equation 1 with Equation 2 and Equation 3, respectively, yields  $V_{CONV\_RESULT}$  in terms of  $V_{SIG\pm}$  and  $V_{OS}$  as shown in Equation 4.

$$V_{CONV\_RESULT} = ([V_{SIG+} - (V_{SIG-} + V_{OS})] - [V_{SIG-} - (V_{SIG+} + V_{OS})]) / 2 \quad (4)$$

Reducing Equation 4 and combining similar terms yields a final conversion result (Equation 5) that is independent of  $V_{OS}$ , which is the desired outcome.

$$V_{CONV\_RESULT} = 2 \times (V_{SIG+} - V_{SIG-}) / 2 = V_{SIG+} - V_{SIG-} \quad (5)$$

### Two-Wire versus Four-Wire AC Excitation

While the previous section shows how to implement AC excitation using all four ACX pins on the ADS1235, it is possible to use only two of the ACX pins to implement AC excitation. Figure 5 shows the modifications required to implement 2-wire AC excitation using the ADS1235.

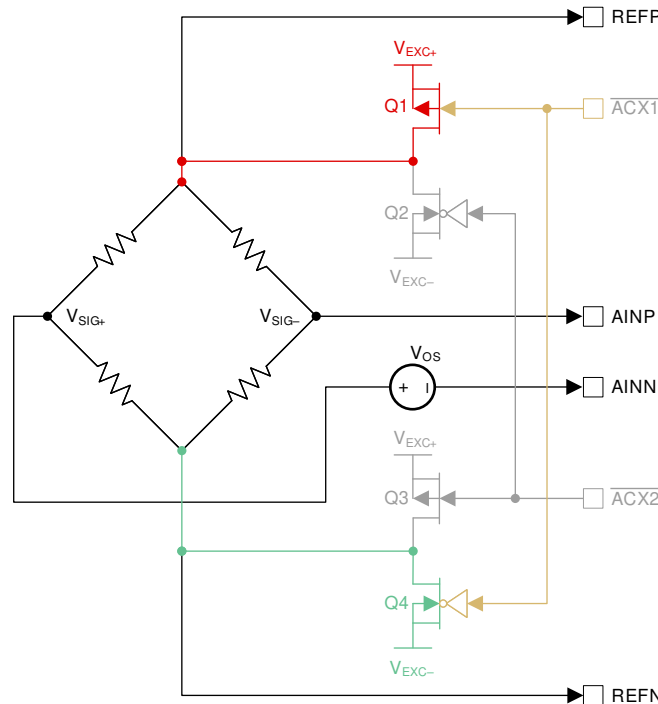


Figure 5. Phase 1 Connection Diagram for 2-Wire AC Excitation

In Figure 5, only the  $\overline{ACX1}$  and  $\overline{ACX2}$  pins are used.  $\overline{ACX1}$  is connected to Q1 and Q4 while  $\overline{ACX2}$  is connected to Q2 and Q3. The addition of two inverters on Q2 and Q4 effectively mimics the 4-wire timing diagram behavior shown in Figure 3. For example, Figure 3 shows that when  $\overline{ACX1}$  is in the forward-polarity, on-switch position,  $\overline{ACX1}$  is logic low. This turns Q1 on, while at the same time the inverted input (logic high) is applied to Q4, turning this MOSFET on as well.

While not shown, the 2-wire AC excitation reverse-polarity phase is the behavioral opposite of the forward polarity phase, similar to the 4-wire case (see Figure 4B). Moreover, the phase and conversion result equations are the same as described in the previous section.

### Example AC Excitation Circuit on the ADS1235 EVM

The ADS1235 evaluation module (EVM) includes an AC excitation circuit that uses a dual-channel gate driver instead of individual MOSFETs to control the bridge. The gate driver used on the EVM is the Texas Instruments UCC27524, a non-inverting device, though it is possible to use the inverting UCC27523 as well. The block diagrams for both devices are shown in Figure 6.

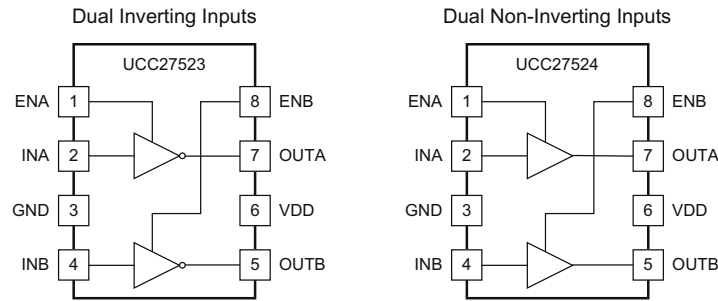


**Figure 6. UCC27523 (Inverting) and UCC27524 (Non-inverting) Block Diagrams**

The UCC27524 operates by driving its OUTx pins to the supply voltage (VDD) when a logic-high input ( $\geq 2.1$  V typical) is applied to INx, or to GND when a logic-low input ( $\leq 1.2$  V typical) is applied to INx. The INx pin voltages are independent of VDD, enabling a dedicated  $V_{EXC\pm}$  that can be greater than the maximum AVDD of 5 V for the ADS1235. This can be used to improve bridge dynamic range if  $V_{EXC\pm} = VDD = 10$  V for example, though there is a tradeoff of higher power consumption and potential sensor self-heating. Moreover, take care to ensure that any voltages applied to the ADC are within the specified operating conditions.

Figure 7 shows the portion of the EVM schematic that contains the AC excitation circuitry, including the UCC27524.

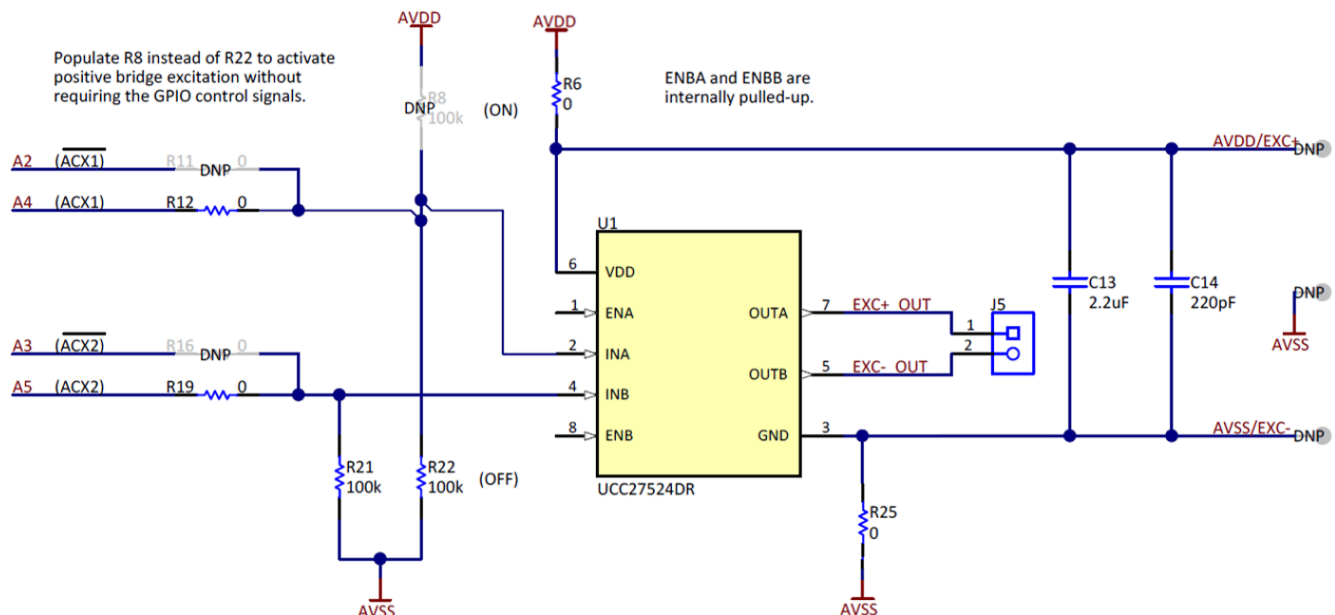


**Figure 7. AC Excitation Circuit on the ADS1235 EVM**

As Figure 7 shows, only two of the four ACX pins are required to implement AC excitation on the ADS1235 EVM. ACX1 and ACX2 are used with the non-inverting UCC27524 that comes standard on the EVM. Comparatively,  $\overline{ACX1}$  and  $\overline{ACX2}$  are used if the UCC27524 is replaced with the inverting UCC27523, which also requires adding resistors R11 and R16 and removing R12 and R19. In either case, the gate driver output is connected to J5-1 and J5-2, which in turn are connected to  $V_{EXC+}$  and  $V_{EXC-}$ , respectively, on an external bridge.

During the forward polarity phase in the circuit in Figure 7, ACX1 is at logic high and ACX2 is at logic low, which sets  $V_{EXC+}$  to AVDD and  $V_{EXC-}$  to GND, respectively. During the reverse-polarity phase of the measurement, ACX1 is at logic low and ACX2 is at logic high, which sets  $V_{EXC+}$  to GND and  $V_{EXC-}$  to AVDD, respectively. Refer to the timing diagram in Figure 3 for more information on the logic levels of each pin during each phase.

After each phase is complete, the ADS1235 takes one measurement and then automatically averages both measurements together pursuant to Equation 2 through Equation 5. The ADS1235 EVM GUI then provides one conversion result with the system-level offset effectively removed.

## Simplifying AC Excitation with the ADS1235

While the AC excitation control circuitry integrated into the ADS1235 can drive external switching components to reverse the polarity of the bridge, this ADC offers additional features to ensure reliable operation.

For example, Phase 2 reverses the excitation voltages such that  $V_{\text{EXC}+}$  and  $V_{\text{EXC}-}$  are connected to REFN and REFP, respectively, resulting in a negative differential reference voltage,  $V_{\text{REF}}$  (see [Figure 4B](#)). Since the ADS1235 cannot support a negative  $V_{\text{REF}}$ , the ADC automatically reverses REFP and REFN during Phase 2 such that a positive  $V_{\text{REF}}$  is always applied to the ADC. Using an ADC without this functionality requires manual  $V_{\text{REF}}$  reversal.

As was discussed previously, the ADS1235 operation also ensures non-overlapping output drive signals, avoiding any MOSFET shoot-through current that could result if both a P-channel and N-channel device were on at the same time (refer to  $t_{d(\text{ACX})}$  in [Figure 3](#)). Moreover, the AC excitation chop rate is synchronized to the conversion data rate to avoid unnecessarily fast switching.

## Additional Considerations for AC Excitation

As with any additional circuitry added to a system, there is a performance tradeoff associated with implementing AC excitation: the improvement in system accuracy requires two measurements to generate one conversion result, thereby increasing conversion time. This doubles the conversion latency values shown in the *Conversion Latency* table in the [ADS1235 Precision, 3-Channel, Differential-Input, 7200-SPS, 24-Bit Delta-Sigma ADC for Bridge Sensors](#) data sheet when AC excitation is enabled. Fortunately, this latency only applies to the first conversion, as subsequent conversions average the previous result with the current result to provide the chopped output value.

Moreover, an added benefit of AC excitation is that the averaging of two measurements reduces the noise performance by a factor of  $\sqrt{2}$ . Therefore, the noise values in the *Noise and Effective Resolution* table in the [ADS1235 data sheet](#) can be divided by 1.41 when AC excitation is enabled.

## Conclusion

Bridge measurements require both precise and accurate systems. The ADS1235 and ADS1261 from Texas Instruments are low-noise, high-accuracy delta-sigma ADCs that integrate control signals for AC excitation circuitry to help reduce system-level offset and offset drift.

## IMPORTANT NOTICE AND DISCLAIMER

TI PROVIDES TECHNICAL AND RELIABILITY DATA (INCLUDING DATASHEETS), DESIGN RESOURCES (INCLUDING REFERENCE DESIGNS), APPLICATION OR OTHER DESIGN ADVICE, WEB TOOLS, SAFETY INFORMATION, AND OTHER RESOURCES "AS IS" AND WITH ALL FAULTS, AND DISCLAIMS ALL WARRANTIES, EXPRESS AND IMPLIED, INCLUDING WITHOUT LIMITATION ANY IMPLIED WARRANTIES OF MERCHANTABILITY, FITNESS FOR A PARTICULAR PURPOSE OR NON-INFRINGEMENT OF THIRD PARTY INTELLECTUAL PROPERTY RIGHTS.

These resources are intended for skilled developers designing with TI products. You are solely responsible for (1) selecting the appropriate TI products for your application, (2) designing, validating and testing your application, and (3) ensuring your application meets applicable standards, and any other safety, security, or other requirements. These resources are subject to change without notice. TI grants you permission to use these resources only for development of an application that uses the TI products described in the resource. Other reproduction and display of these resources is prohibited. No license is granted to any other TI intellectual property right or to any third party intellectual property right. TI disclaims responsibility for, and you will fully indemnify TI and its representatives against, any claims, damages, costs, losses, and liabilities arising out of your use of these resources.

TI's products are provided subject to TI's Terms of Sale (<https://www.ti.com/legal/termsofsale.html>) or other applicable terms available either on [ti.com](https://www.ti.com) or provided in conjunction with such TI products. TI's provision of these resources does not expand or otherwise alter TI's applicable warranties or warranty disclaimers for TI products.

Mailing Address: Texas Instruments, Post Office Box 655303, Dallas, Texas 75265  
Copyright © 2021, Texas Instruments Incorporated